The FEBS Journal

FEBS PRESS science publishing by scientists

The atypical sphingosine 1-phosphate variant, d16:1 S1P, mediates CTGF induction via S1P2 activation in renal cell carcinoma

Melanie Glueck[1], Alexander Koch[1], Robert Brunkhorst[2], Nerea Ferreiros Bouzas[3], Sandra Trautmann[3], Liliana Schaefer[1], Waltraud Pfeilschifter[1,4], Josef Pfeilschifter[1] and Rajkumar Vutukuri[1]

1 Institute of General Pharmacology and Toxicology, University Hospital and Goethe University Frankfurt, Germany
2 Department of Neurology, University Hospital, RWTH Aachen, Germany
3 Institute of Clinical Pharmacology, University Hospital and Goethe University Frankfurt, Germany
4 Department of Neurology, Klinikum Lueneburg, Germany

Keywords
A498 cells; CTGF; RCC; S1P receptors; sphingosine 1-phosphate homologues

Correspondence
R. Vutukuri and M. Glueck, Institute of General Pharmacology and Toxicology, University Hospital and Goethe University Frankfurt, Frankfurt am Main, Germany
Tel: +49 (0)69 6301 6959
E-mails: vutukuri@med.uni-frankfurt.de (RV); m.glueck@blutspende.de (MG)

(Received 30 August 2021, revised 2 February 2022, accepted 22 March 2022)

doi:10.1111/febs.16446

Sphingosine 1-phosphate (S1P) is a lipid mediator with numerous biological functions. The term 'S1P' mainly refers to the sphingolipid molecule with a long-chain sphingoid base of 18 carbon atoms, d18:1 S1P. The enzyme serine palmitoyltransferase catalyses the first step of the sphingolipid *de novo* synthesis using palmitoyl-CoA as the main substrate. After further reaction steps, d18:1 S1P is generated. However, also stearyl-CoA or myristoyl-CoA can be utilised by the serine palmitoyltransferase, which at the end of the S1P synthesis pathway, results in the production of d20:1 S1P and d16:1 S1P respectively. We measured these S1P homologues in mice and renal tissue of patients suffering from renal cell carcinoma (RCC). Our experiments highlight the relevance of d16:1 S1P for the induction of connective tissue growth factor (CTGF) in the human renal clear cell carcinoma cell line A498 and human RCC tissue. We show that d16:1 S1P versus d18:1 and d20:1 S1P leads to the highest CTGF induction in A498 cells via S1P2 signalling and that both d16:1 S1P and CTGF levels are elevated in RCC compared to adjacent healthy tissue. Our data indicate that d16:1 S1P modulates conventional S1P signalling by acting as a more potent agonist at the S1P2 receptor than d18:1 S1P. We suggest that elevated plasma levels of d16:1 S1P might play a pro-carcinogenic role in the development of RCC via CTGF induction.

Introduction

Renal cell carcinoma (RCC) is the most common kidney cancer in adults representing more than 90% of the occurrences and emerges from cells lining the renal tubules. RCC is highly metastatic and an aggressive type of cancer that, when metastatic, is resistant to conventional chemotherapy treatment regimes. The proliferation comes from the tubular epithelium and is histologically categorised in the clear cell, papillary and chromophobic renal carcinoma [1]. The tumour microenvironment is characterised by constitutive activation of fibroblasts, epithelial–mesenchymal transition and tumour–stroma interactions [2]. Renal fibrosis is one of the main criteria of all chronic kidney diseases and often occurs in tumours [3,4]. The terminal stage of renal insufficiency is composed of glomerular, vascular and tubulointerstitial fibrosis that strongly

Abbreviations
CNS, central nervous system; CTGF, connective tissue growth factor; FCS, fetal calf serum; LCB, long-chain sphingoid base; RCC, renal cell carcinoma; S1P, sphingosine 1-phosphate; S1P1-5, S1P receptor 1-5; SPT, serine palmitoyltransferase.

The FEBS Journal **289** (2022) 5670–5681

correlates with the failure symptoms of the kidney as well as with the prognosis of the disease [5–7].

Studies showed that the remodelling of the extracellular matrix plays an important role in the increase of tumour proliferation and the formation of metastasis [8,9]. Intratumoural fibrosis and inflammation are frequently observed histological findings in solid tumours. Several studies described intratumoural fibrosis as a negative prognostic factor in cancer [10]. The renal carcinoma also belongs to the highly vascularised tumours, that shows different forms of intratumoural fibrosis [4].

The connective tissue growth factor (CTGF) is an important profibrotic factor, that also plays a major role in connection with kidney diseases [11]. It is a cysteine-rich polypeptide, that, after its secretion into the extracellular matrix, can modulate cell functions via interaction with cytokines and growth factors [12–14]. An increased CTGF expression goes along with cell proliferation and accumulation of components of the extracellular matrix, which could also be observed in inflammatory glomerular and tubulointerstitial diseases of the kidney [15]. Furthermore, several studies were performed that indicate that CTGF plays a role in carcinogenic processes such as the proliferation of hepatocellular carcinoma or peritoneal metastasis of gastric cancer [16,17]. Another recently published study by Okusha et al. [18] provides data about tumour-derived extracellular vesicles that were enriched with fragments of CTGF and turned out to be protumourigenic in mice.

Sphingolipids are structural components of cell membranes and additionally act as bioactive lipid mediators, which for example take part in the regulation and recruitment of various immune cells and their cellular functions [19,20]. They are composed of the amino alcohol sphingosine, which has an amino group and two hydroxy groups. The sphingolipid metabolite sphingosine 1-phosphate (S1P) is characterised by its functional diversity, as it takes part in numerous biological processes, among them cell migration, immune response, cell proliferation and cell survival [19,21]. Therefore it has great relevance in plenty of diseases such as ischemic stroke, atherosclerosis, cancer, autoimmune processes or fibrosis [22–26]. It exerts its effects para- or autocrine via five G protein-coupled receptors (S1P1-5) or at the intracellular level [19,20].

In the *de novo* synthesis of S1P, the enzyme serine palmitoyltransferase (SPT) catalyses the reaction of palmitoyl-CoA and serine to 3-ketosphinganine. After several chemical transformations, the product S1P with a long-chain sphingoid base (LCB) of 18 carbon atoms, d18:1 S1P, is formed. This S1P homolog is the most prevalent and best studied in eukaryotes. The enzyme SPT is composed of a large subunit dimer (SPTLC1 and SPTLC2 or SPTLC3) and a small subunit (SPTssa or SPTssb) [27]. Due to the varying activity of the different subunits, different acyl-CoAs can be preferred as substrates [28,29]. In SPT homologues other determinants of substrate specificity such as substrate-induced conformational changes have been described. This could potentially result in the conversion of other acyl-CoA substrates rather than the mainly used palmitoyl-CoA [30].

A recently published study describes the presence and relevance concerning COX-2 expression of a S1P with a LCB of 20 carbon atoms, d20:1 S1P, in the central nervous system (CNS) of mice and human glioblastoma tissue [31]. Besides that, other S1P homologues of different chain lengths are measurable in human plasma. Wang et al. [32] for example could verify that the concentration of d16:1 S1P in patients undergoing therapy with oxaliplatin is increased. Another study found out that d16:1 S1P is significantly reduced in plasma of patients with vascular dementia and suggests it to play a potential role in fine-tuning of d18:1 S1P-mediated cytokine production [33]. According to Hornemann et al. [29] overexpression of the SPT subunit SPTLC3 leads to the production of sphingoid bases with 16 carbon atoms. Until now, there are few investigations about S1P receptor activation by d16:1 S1P [32,34], while hardly any data have been published to explain its physiological role. The studies mentioned, implicate a functional relevance of S1P homologues of different chain lengths. However, even though fine adjustment in the production of S1P derivates of different chain lengths might serve the maintenance of balance that can be of great importance for the destiny of the cell, very few investigations have been made on this subject so far [35].

This study aims to investigate a possible role of the chain length of S1P concerning signalling pathways in renal carcinoma cells, suggesting chain length dependent effects of S1P signalling on physiological regulatory mechanisms. Therefore, S1P homologues with LCBs of 16, 18 and 20 carbon atoms were used *in vitro* and their effects on receptor activation and CTGF-protein expression were analysed. Furthermore, we investigated the concentration of the mentioned S1P homologues in different organs in mice as well as in human patient samples of RCC.

Results

Distribution of S1P homologues with different chain lengths in mice and elevated levels of d16:1 and d18:1 S1P in human RCC tissue

The emergence of the role of sphingolipids, especially S1P, in health and diseases is being increasingly

recognised, whereas the contribution of different chain lengths of S1P in vertebrates remains to be unravelled. Recently, we published our findings on the distribution and functions of d20:1 S1P in human glioblastoma samples and LN229 cell line respectively. In the current study, we investigated the occurrence of d16:1 S1P in mice followed by the significance in human RCC tissue and cell line A498.

At first, employing the LC-MS/MS method with reference lipids, we measured the levels of d16:1 S1P in kidneys and various organs along with S1P homologues of other long-chain bases. Regarding d20:1 S1P, our previous results in the CNS of mice could be confirmed. We could detect d16:1 S1P in kidneys (Fig. 1A) and most of the peripheral organs except thymus, heart and retina whereas d20:1 S1P was measurable in all organs. (Fig. 1C). In all compartments, the extent of d18:1 S1P is beyond 10- to 100-fold compared to the other S1P homologues including the CNS (Fig. 1A–D). The highest amount of d16:1 S1P was detected in the cerebellum (Fig. 1D; 30.8 ± 9.5 pg·mg^{-1}). Interestingly, plasma and serum of mice encompassed higher levels of d16:1 S1P than d20:1 S1P (Fig. 1B; d16:1 S1P vs. d20:1 S1P; 245.5 ± 32.3 pg·mg^{-1} vs. 1.7 ± 8.0 pg·mg^{-1}; P-value < 0.05). The levels of d20:1 Sphingosine and Sphiganine in mice kidneys were below the level of detection limit whereas, in case of d16:1, they were not measured (n.m.) due to the non-availability of standards (Fig. 1A).

To validate the physiological relevance, we additionally analysed the levels of d16:1 S1P along with other LCBs in human renal carcinoma and control tissue of patients obtained from the University Cancer Centre (UCT), Frankfurt. We detected elevated levels of d16:1 S1P (Fig. 1E; Control vs. RCC; 13.1 ± 13.2 pg·mg^{-1} vs. 29.1 ± 23.8 pg·mg^{-1}; P-value < 0.05) and d18:1 S1P (Fig. 1E; Control vs. RCC; 30.1 ± 30.3 pg·mg^{-1} vs. 70.1 ± 57.3 pg·mg^{-1}; P-value < 0.05) in a significant number of tumour samples in comparison to the corresponding controls. Also, other sphingolipid metabolites such as sphingosine and sphinganine of C18 and C20 LCB origin were raised in tumour tissues (Fig. 1E). Due to the non-availability of standards for sphingosine and sphinganine of C16 LCB these measurements could not be performed.

d16:1 S1P induced CTGF to a higher extent than d18:1 S1P in A498 renal carcinoma cell line

Recent literature implicated the role of CTGF in tumour progression and vast evidence accorded d18:1 S1P to induce CTGF [2,17,18]. We aimed to investigate if d16:1- and d20:1 S1P induce CTGF in RCC using the renal clear cell carcinoma cell line A498 *in vitro*. Our results manifested a chain length dependent elevation of CTGF mRNA [Fig. 2A; d16:1 S1P: 355.6 ± 105.4 (fold expression of Gapdh); d18:1 S1P 259.9 ± 93.3 (fold expression of Gapdh), P-value < 0.05] and protein expression (Fig. 2B,C) by different S1P homologues, where the shortest chain length d16:1 displayed the highest CTGF induction followed by d18:1 after 2 h of treatment with the respective lipid. d20:1 S1P did not lead to a significant CTGF mRNA induction compared to an untreated control. Besides, a combination treatment of d18:1- and d16:1 S1P led to a further increase in CTGF mRNA expression but not at protein level (Fig. 2A–C). Furthermore, to check the main contributor of the CTGF induction, we admixed d16:1- or d18:1 S1P with different concentrations of either d18:1- or d16:1 S1P respectively. The combination treatment of d18:1- and d16:1 S1P led to a higher induction of CTGF mRNA than the single treatment with d18:1 S1P. This effect appeared only at a concentration of d16:1 S1P of 1 μM and not when lower concentrations of d16:1 S1P were used (Fig 2F). Also, we performed the dose-dependent activation of CTGF in A498 cells upon treating with homologues of S1P of different chain lengths. The results corroborated that d16:1- and d18:1 S1P dose-dependently increased mRNA expression of CTGF 2 h after treatment in A498 cells while d20:1 S1P did not show significant induction of CTGF mRNA expression (Fig. 2D). We also performed time-course experiments (0.5, 1, 2, 4, 8, 24 h) in the A498 cell line and our data revealed that CTGF mRNA induction is highest after 2 h compared to other time points in case of treatment with all S1P homologues (Fig. 2E).

Induced CTGF, S1P2 and S1P3 expression in human renal carcinoma tissues

To check our results in human conditions, we also verified the changes in CTGF expression in human RCC tissue samples using mRNA [Fig. 3A; Control vs. RCC; 8.3 ± 25.9 vs. 14.5 ± 40.1 (fold expression of HPRT1), P-value < 0.05] expression and Western blot analysis (Fig. 3B,C). Both revealed a significant increase of CTGF in tumour samples in comparison to control (Fig. 3A–C). In the majority of the tumour tissue samples, our Western blot experiments and their quantification evinced the upregulation of S1P2 and S1P3 receptor protein significantly compared to the corresponding healthy tissue (Fig. 3D–G) but not that of the other S1P receptors (data not shown). It is well

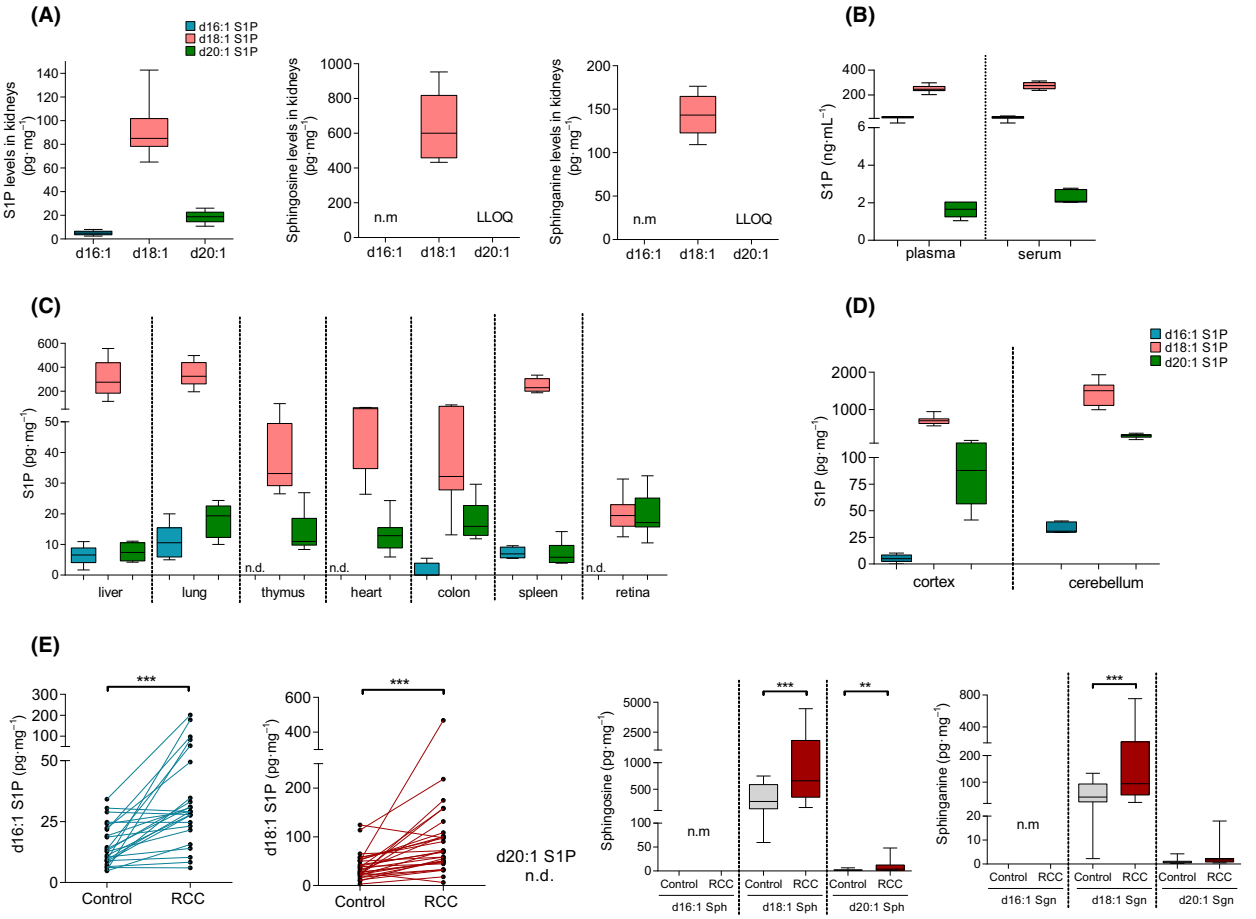

Fig. 1. Occurrence of different S1P homologues in mice and renal cell carcinoma samples. S1P, sphingosine and sphinganine levels measured in kidneys of male C57BL/6J mice (A). S1P levels were measured in plasma and serum (B), different organs (C) and brain tissue (D) of male C57BL/6J mice. S1P, sphingosine and sphinganine levels were measured in the tissue of human patients with clear cell renal carcinoma (E) by LCMS/MS as described in the section Material and Methods. (A–D): Data are shown as median ± IQR (n = 5–10, samples measured from three independent measurements). (E): The levels of d16:1 S1P and d18:1 S1P are higher in 20 out of 25 and 28 out of 29 RCC samples compared to respective controls (non-tumourous kidney tissue from the same patient) (n = 25–29, samples measured from three independent experiments). Sphingolipids not measured due to commercially non-availability of standards are indicated as n.m. (not measured) and LLOQ implies a Lower limit of quantitation of the LCMS analysis. Wilcoxon matched-pairs signed-rank test was used for measuring significance in case of human samples. $^{**}P < 0.01$, $^{***}P < 0.001$, n.d implies not detectable in LCMS/MS measurements.

documented that S1P signalling, which predominantly occurs through S1P1-5 G protein-coupled receptors is involved in CTGF activation. To understand the mechanism of CTGF activation by d16:1- and d18:1 S1P we investigated the occurrence of S1PR1-5 and alterations in receptor expression in the A498 cell line and RCC tissue samples respectively. Our mRNA analysis revealed the expression of all five S1P receptors in both tumour tissue (data not shown) as well as in the A498 cell line (Fig. 4A). Regarding general expression, in A498 cells, the S1P3 receptor mRNA has the highest presence, followed by S1P5 (Fig. 4A). These findings strengthen our hypothesis that the production of CTGF, which is increased in the RCC samples compared to healthy tissue, might be linked to either S1P2 or S1P3 signalling.

S1P2 but not S1P3 inhibition leads to the reduction of CTGF in renal carcinoma cells

Previous studies have published evidence connecting S1P2 and S1P3 receptors to be responsible for the activation of the proliferative CTGF [16,36,37]. Hypothesising the role of S1P2 and S1P3 receptors as being most likely responsible for CTGF induction in A498 cells and because they were upregulated in the tissue of RCC, we concentrated our mechanistic studies on these two receptors. Therefore, we co-stimulated A498 cells with

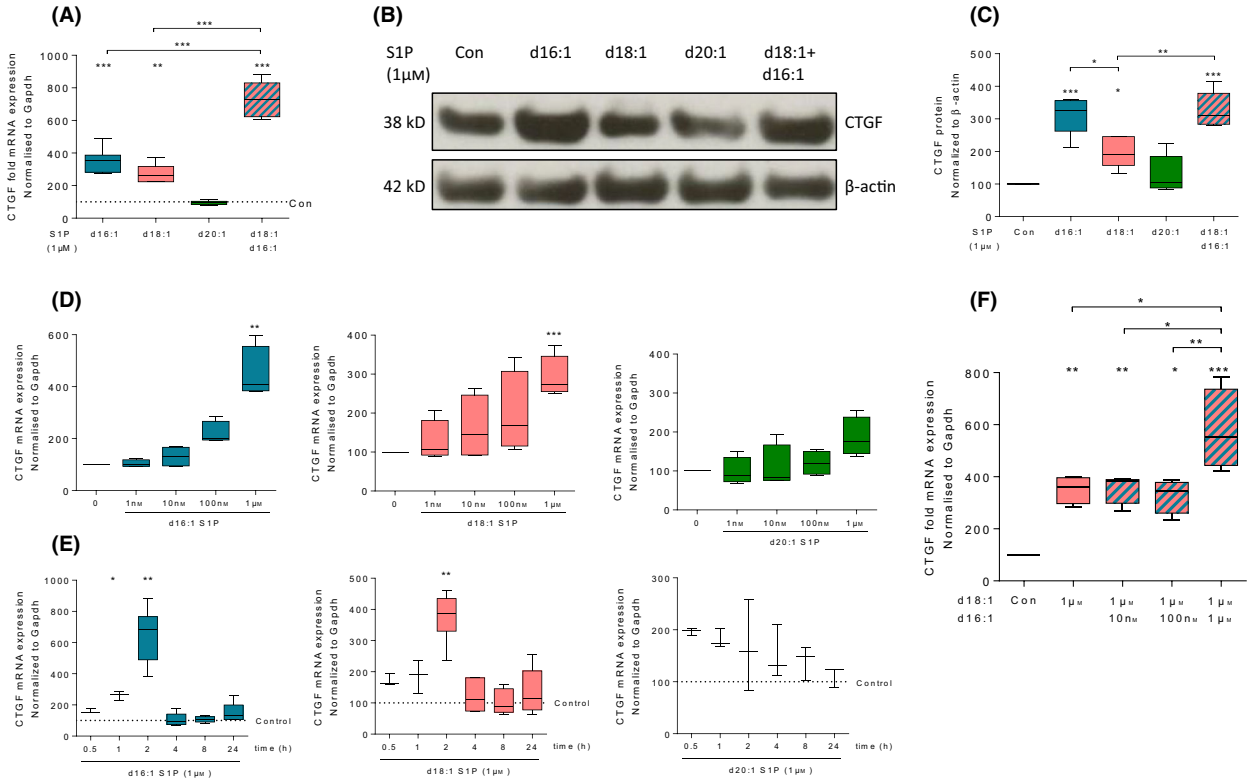

Fig. 2. d16:1 S1P has the highest capability of CTGF induction compared to d18:1- and d20:1 S1P in A498 cells. Effect of d16:1-, d18:1- and d20:1 S1P on the expression of CTGF mRNA (A) and protein (B, C) in A498 cells. Cells were stimulated for 2 h with 1 μM d16:1-, d18:1-, d20:1 S1P or both d16:1 S1P + d18:1 S1P. CTGF mRNA and protein expression were measured by TaqMan® and Western blot analysis as described in the section Materials and Methods. Concentration-dependent effect of d16:1-, d18:1- and d20:1 S1P (D). Cells were stimulated for 2 h with 1 nM, 10 nM, 100 nM or 1 μM S1P as indicated. Time-dependent effect of d16:1-, d18:1- and d20:1 S1P (E). Cells were stimulated for 0.5, 1, 2, 4, 8 or 24 h with the respective S1P homologues as indicated. mRNA induction of CTGF with 1 μM d16:1 S1P or 1 μM d18:1 S1P alone or in combination with increasing doses of d16:1 S1P (0.01 μM, 0.1 μM and 1 μM) (F). All experiments were conducted three to five times with one to two samples in each experiment. Data are shown as median ± IQR. $*P < 0.05$, $**P < 0.01$, $***P < 0.001$.

either the S1P2 inhibitor JTE-013 or the S1P3 and S1P1 inhibitor VPC23019, respectively, together with d16:1- or d18:1 S1P for 2 h and analysed mRNA and protein expression of CTGF (Fig. 4B–G). Our results exhibited pronounced inhibition of CTGF protein as well as mRNA expression in A498 cells with 10 μM JTE-013 (Fig. 4B–D), whereas co-stimulation with 10 μM VPC23019 (Fig. 4E–G) disposed no effect affirming our hypothesis that S1P2 mediates CTGF induction in renal clear cell carcinoma line A498. The blocking of CTGF mRNA and protein expression was significant in both d16:1 + JTE-013 [Fig. 4B; d16:1 S1P vs. d16:1 S1P + JTE-013, 496.5 ± 355.9 vs. 246.8 ± 87.1 (fold expression of Gapdh) P-value < 0.05] as well as d18:1 + JTE-013 treatment paradigms (Fig. 4B–D). In contrast, the protein intensity of CTGF was markedly elevated in the co-stimulation of d18:1 with VPC23019 (Fig. 4E–G) offering a hint that S1P3 might be involved in checking the activation of CTGF by modulating the final response of the receptor. Another possibility would be that by blocking the S1P1 and S1P3 receptors, more S1P binds to the S1P2 receptor leading to an increase in CTGF production. As till date, there is no data available, that would explain this behaviour, further studies on this subject would be interesting. Finally, we availed PRESTO-Tango reporter assay to deduce the ability of S1P homologues to activate S1P2 and S1P3 receptor subtypes (Fig. 4H). There is little literature available about the activation of S1P receptors by d16:1 S1P. Our luciferase assay confirmed that like d18:1 S1P the shorter chain length S1P homologue d16:1 S1P also activates the S1P2 and S1P3 receptors (Fig. 4H). Also, the S1P2 and S1P3 luciferase activity was highest when treated with d16:1 S1P [Fig. 4H; 1291 ± 1929.3 (fold expression of control), P-value < 0.05] compared to other homologues (Fig 4H). Overall, our results

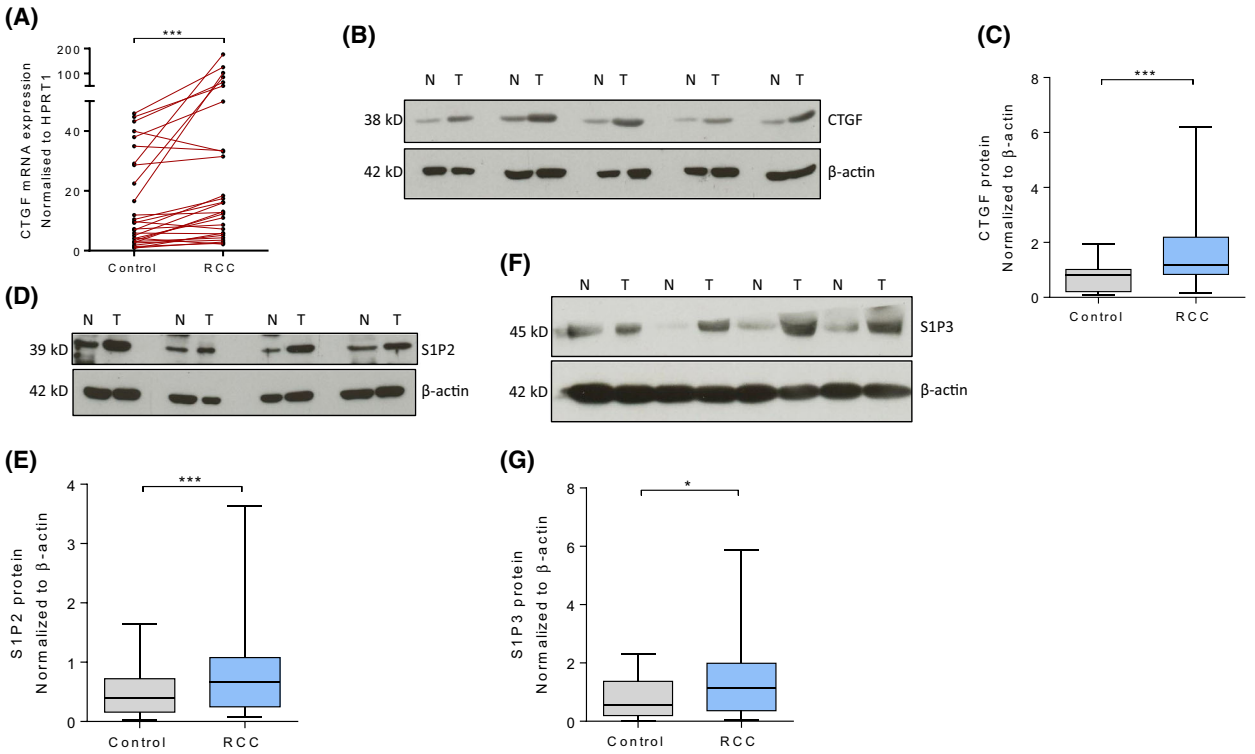

Fig. 3. CTGF mRNA and protein expression is induced in human RCC patient samples. S1P2 and S1P3 receptor protein levels are upregulated in human RCC patient samples. CTGF mRNA (A) and protein expression (B, C) measured in RCC and corresponding healthy renal tissue as described in the section Materials and Methods. Data are shown as median ± IQR. ***$P < 0.001$ ($n = 28$ human RCC patient samples) 24 out of 28 RCC samples had higher CTGF mRNA expression in comparison to respective controls (non-tumourous kidney tissue from the same patient). S1P2 (D, E) and S1P3 (F, G) protein levels were analysed by Western blot as described in Materials and Methods. Data were analysed by measuring the band intensity in comparison to healthy tissue of the same patient using ImageJ software (A–E: $n = 25$–28 samples). Western blot images shown above are representative images for 4 controls and RCC samples. *$P < 0.05$, ***$P < 0.001$.

demonstrate that d16:1- and d18:1 S1P homologues might play a role in RCC via enhancing CTGF protein expression. Based on the results of our antagonistic studies, we conclude that CTGF induction is most likely activated by the S1P2 receptor.

Discussion

This study aimed to characterise the role of S1P homologues of different chain lengths in renal cancer. We first re-evaluated the concentrations of d18:1- and d20:1 S1P and also measured d16:1 S1P in mice and RCC tissue. We show that levels of d16:1-, d18:1 S1P and CTGF are increased in RCC compared to healthy tissue. Functionally, d16:1 S1P and d18:1 S1P can induce CTGF upregulation in the renal clear cell carcinoma cell line A498 most likely via S1P2. We identify d16:1 S1P as the most potent agonist on the S1P2 receptor compared to the other S1P homologues used, suggesting that d16:1 S1P might have carcinogenic potential or influence RCC prognosis via CTGF-induced fibrosis.

Our results show that d18:1 S1P is the predominant S1P homologue in all organs of mice as well as in human RCC tissue. We could confirm the presence of other S1P homologues as described by others [32,34,38], showing that also d16:1- and d20:1 S1P were detectable in the majority of organs of mice; d16:1 S1P was additionally measured in the RCC samples. Performing luciferase assay of the S1P2 and S1P3 receptors, d16:1 S1P turned out to be the most potent agonist of the S1P2 receptor compared to d18:1- and d20:1 S1P. In this aspect, our findings contradict a study published by Troupiotis-Tsailaki et al. [34] that postulates d20:1 S1P as the most potent ligand of the S1P2 receptor followed by other S1P homologues that show a lower receptor activation potential with decreasing chain length. Wang et al. [32] also describe d16:1 S1P to have a lower efficacy on the S1P2 receptor compared to d18:1 S1P. The differing results could

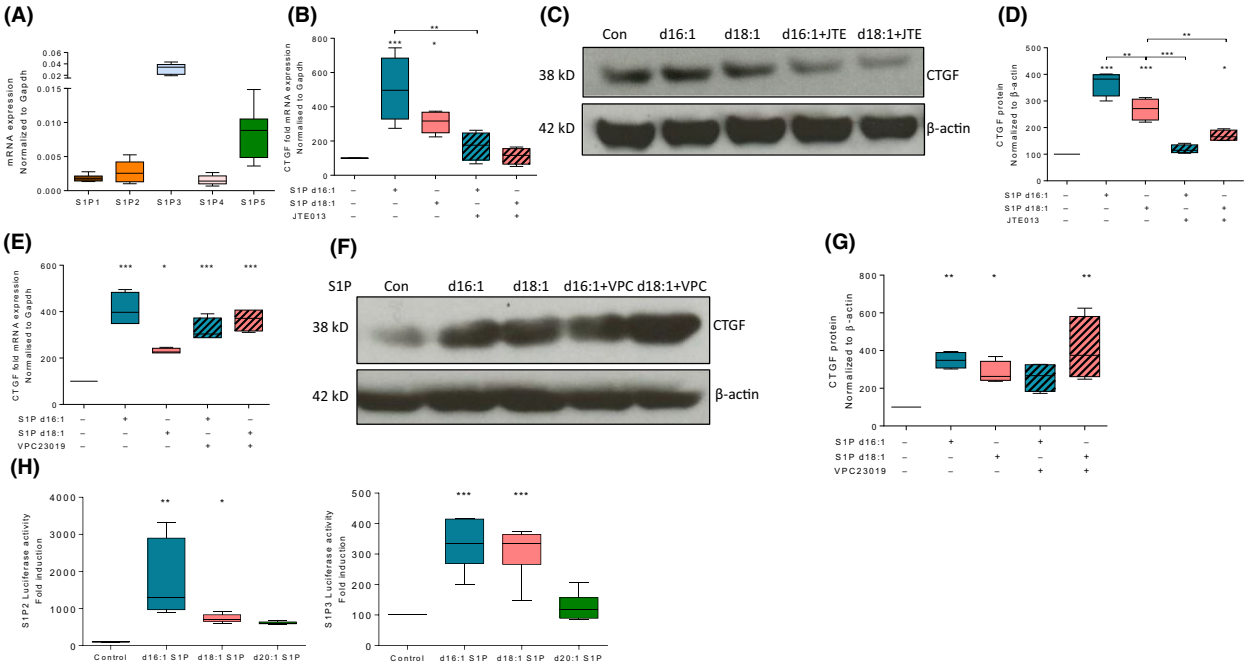

Fig. 4. S1P-mediated CTGF induction blocked by S1P2 inhibitor JTE-013 but not S1P3 inhibitor VPC23019, S1P2 and S1P3 receptor activation by different S1P homologues. S1P receptors mRNA expression in A498 cells measured by TaqMan® (A). d16:1, d18:1 and d20:1 S1P dependent CTGF mRNA and protein expression followed by treatment with JTE-013 (B–D) and VPC23019 treatments (E–G) in A498 cells. Cells were stimulated for 2 h with 1 μM d16:1-, d18:1- or d20:1 S1P in the absence or presence of 10 μM JTE-013 or VPC23019. CTGF mRNA and protein expression were measured by TaqMan® and Western blot analysis as described in the section Material and Methods. Luciferase activity is induced by activation of S1P2 and 3 receptors (H). Cells were treated for 17 h with either vehicle, 1 μM d16:1-, d18:1- or d20:1 S1P as indicated. All experiments were conducted four to five times with one to two samples in each experiment. Data are shown as median ± IQR. $*P < 0.05$, $**P < 0.01$, $***P < 0.001$.

be explained by the different methods and cell lines that were used to measure receptor activity. Troupiotis-Tsailaki et al. [34] used the aequorin-based calcium mobilisation assay in CHO-L1 cells and Wang et al. [32] made use of the TGFα-shedding assay in HEK293 cells. We, on the other hand, performed the PRESTO-Tango luciferase assay in HTLA cells which, compared to the other assays mentioned above, determines direct receptor activation. Moreover, the results in our mRNA experiments in A498 cells show the higher CTGF induction by d16:1- than by d18:1 S1P, which was significantly reduced by the S1P2 receptor inhibitor JTE-013. This strengthens our hypothesis that the agonistic potential of d16:1 S1P on the S1P2 receptor is higher in comparison to d18:1 S1P.

Vutukuri et al. [31] observed that d20:1 S1P can inhibit d18:1 S1P-induced S1P2 receptor activity, suggesting a partial antagonism of d20:1 S1P at that receptor. Our data indicated that co-stimulation of d16:1- and d18:1 S1P lead to a significantly higher S1P2 receptor activity than d18:1 S1P alone. This led to the assumption that different S1P homologues might have chain length dependent agonistic potential at S1P receptors. The data goes along with the findings of Maeda et al. [39] showing that S1P homologues with shorter lipid tails than d18:1 induce $G_{12/13}$- and $G_{i/o}$-biased signalling via the S1P3 receptor, whereas d18:1 S1P can additionally activate $G_{q/11}$ via the S1P3 receptor.

Troupiotis-Tsailaki et al. [34] describe, that with an increasing chain length of the fatty acid of S1P, the receptor activation potential increases. As an underlying mechanism to this phenomenon, they propose that the affinity of S1P for its receptor depends on polar interactions between the head group of the lipid and side chains of the receptor. Responsible for the activation of the receptor is an interaction of the hydrophobic lipid tail with a specific binding site of the receptor. In case of the S1P2 receptor, our data do not confirm the statement of Troupiotis-Tsailaki et al. [34], as the activation potential decreases with an increasing chain length of the S1P homologue (Fig. 4H).

It is already well known, that d18:1 S1P leads to an upregulation of various proteins, including CTGF. This protein is known to act profibrotic, playing a role in the development of kidney fibrosis [40], but also

acts in a pro-tumourigenic way [2,16–18]. Cheng et al. [16] recently published, that S1P promotes the proliferation of hepatocellular carcinoma via an S1P2 receptor-mediated CTGF upregulation. Errarte et al. [2] described that cancer-associated fibroblasts recruitment and activation of CTGF among others play an important role in many malignant neoplasms, for example, RCC. Additionally, Lv et al. [17] reported that transforming growth factor β_1 by inducing CTGF, promotes peritoneal metastasis of gastric cancer.

On a functional level, we investigated the effects of S1P homologues of different chain lengths on the expression of CTGF, as currently there is little data available on this subject. As our results showed elevated levels of CTGF in RCC compared to healthy kidney tissue, our data might be another hint for CTGF's pro-carcinogenic potential. The fact, that also d16:1- and d18:1 S1P levels were increased in the tumour tissue in such a way that levels of d16:1 S1P even reached the levels of d18:1 S1P and that both lipids lead to the upregulation of CTGF in the human renal cancer cell line, confirms the pre-existing assumption that S1P induces CTGF [40,41]. This additionally suggests, that chain length-dependent signalling pathways also play a role in CTGF expression as mRNA levels of CTGF were higher after stimulation with d16:1- than with d18:1 S1P and not present after incubation with d20:1 S1P. By blocking the S1P2 receptor in A498 cells, we proved that the CTGF pathway is, at least partly, S1P2-dependent, which goes along with previously provided data [16,36]. The higher activation of the S1P2 receptor by d16:1- compared to d18:1 S1P and the fact that the S1P2 receptor was upregulated in the RCC tissue, suggests that d16:1 S1P could partly be responsible for tumour proliferation via CTGF upregulation. In this aspect, our data partly disagree with Chua et al. [33], who postulate d16:1- and d18:1 S1P as inductors of pro-inflammatory cytokines. In contrast, they showed, that d16:1 S1P reduced the pro-inflammatory effects of d18:1 S1P. In a previous analysis [31], we showed, that d20:1 S1P can inhibit a d18:1 S1P-induced COX-2 upregulation in glioblastoma cells. Interestingly, co-stimulation with d16:1- and d18:1 S1P led to an increased S1P2 activity compared to incubation with d18:1 S1P alone (data not shown). On the other hand, the presence of higher concentrations of d16:1 S1P but not d18:1 S1P enhanced CTGF and the maximum induction of CTGF did not rise beyond the d16:1 S1P (1 μM) treatment alone. That is why we would expect higher levels of d16:1 S1P to potentiate CTGF expression probably because of stronger receptor activation. It should be mentioned, that in case of the RCC samples, S1P levels were measured in control tissue collected nearby the tumour, so that real health conditions might not be represented by our data. Tissue that is surrounded by malignant tissue, could also underlie fibroblast activation and therefore produce higher amounts of CTGF. It is difficult to represent true health conditions since biopsies are rarely performed from healthy organs. An animal model in which the contralateral kidney that is not infiltrated by malignant tissue is observed, would be interesting.

Mechanistically, a similar affinity but lower efficacy of S1P homologues of different chain lengths could be the reason for their different agonistic potential at the different receptors [31,42]. This would also support the hypothesis that the polar head group of S1P is responsible for its affinity at the receptor, while the chain length of the fatty acid component determines the degree of activation of the receptor [42].

There are already data, that suggest therapeutic effects of S1P, for example, in connection with the development of renal fibrosis [43]. Ren et al. [44] for example, explain the antifibrotic effects of intracellular formed S1P via a reduction of CTGF production in podocytes. Koch et al. [45] were able to observe this effect in human mesangial cells and mice. On the other hand, S1P which stimulates the cell from extracellular has profibrotic effects via increased CTGF expression [41]. These research results suggest that S1P can influence CTGF production through different signalling pathways. Our data offer a modulation option for the signalling cascade triggered by S1P, which has so far not been carefully addressed. The fact, that d16:1 S1P is the strongest inducer of CTGF mRNA expression and is also upregulated in RCC tissue, could be a hint that increased plasma levels of d16:1 S1P might be a risk factor for the development of renal cancer. In our study, we used high doses of S1P as a proof of concept to reach sufficient receptor activation. In the future, *in vivo* studies will be necessary to strengthen our data as it is very difficult to replicate compartmental differences and turnover effects that can affect signalling *in vitro*. We assume, that physiological levels of d16:1 S1P under homeostatic conditions do not account for higher CTGF expression and that there might be controlling mechanisms to inhibit d16:1 S1P production. A future study, in which the corresponding plasma levels in patients who suffer from renal fibrosis compared to healthy individuals, could provide information on this hypothesis.

In conclusion, our data suggest increased levels of d16:1 S1P to be a potential risk factor of RCC. We propose, that d16:1- and d20:1 S1P might be endogenous modulators of S1P signalling and assume that

the metabolism of S1P homologues of different chain lengths might be an essential part of S1P-signalling. The maintenance of balance of various S1P homologues could significantly contribute to the evolvement of S1P's effects and implications in homeostasis and diseases.

Materials and Methods

Materials

d16:1 S1P, d18:1 S1P and d20:1 S1P were purchased from Avanti polar lipids (Alabaster, AL, USA), JTE-013 was from Cayman Chemicals (Ann Arbor, MI, USA) and VPC23019 was obtained from Tocris biosciences (Bristol, UK). All media and cell culture essentials were purchased from Thermo Fisher Scientific (Darmstadt, Germany).

Cell culture and stimulation

For all *in vitro* experiments in the present study, A498 human clear cell kidney carcinoma cells between passages 10 and 20 were seeded in six-well cell culture plates and grown in Dulbecco's modified Eagle medium (DMEM) containing 10% (v/v) fetal calf serum (FCS) and 1% (v/v) penicillin/streptomycin to confluency. Prior to stimulation, the complete medium was substituted with a minimal medium without FCS overnight. On the next day, cells were treated for 2 h (unless otherwise mentioned) with either d16:1 S1P, d18:1 S1P, d20:1 S1P, JTE-013 or VPC23019 as described in the respective figure legends. All chemicals were dissolved according to manufacturers' instructions.

Real-time PCR analysis of gene expression

For mRNA gene expression analysis, a two-step PCR experiment was done as described previously [46]. RNA was isolated with TRIZOL reagent (Sigma-Aldrich, Steinheim, Germany) and cDNA was transcribed from 1 μg total RNA using RevertAid Reverse Transcriptase kit (Thermo Scientific, Darmstadt, Germany) following manufacturer's protocol. RT-PCR was performed using 2 × qPCRBIO probe mix Lo-ROX (Nippon Genetics, Dueren, Germany). The cycling conditions of the Applied Biosystems 7500 Fast Real-Time PCR System used, were as follows: 95 °C for 2 min (1 cycle), 95 °C for 5 s and 60 °C for 30 s (40 cycles). The following predesigned Taqman probes with reporter dyes 6-FAM or VIC from Thermo Fisher Scientific were utilised: Hs00170014_m1 (for human CTGF), Hs01922614_m1 (for human S1P1), Hs00245464_m1 (for human S1P3), Hs02330084_m1 (for human S1P4), Hs00928195_m1 (for human S1P5), Hs99999905_m1 (for human Gapdh), Hs02800695_m1 (for human HPRT1) and qHsaCEP0024756 (for S1P2 from Bio-rad). Relative changes in the mRNA expression were performed using the $2-\Delta C_t$ or $\Delta\Delta C_t$ method, the threshold cycle (C_t) was calculated by the instrument's software. Gapdh for cell culture experiments and HPRT1 mRNA expression for human samples were used for normalising.

Western blot analysis

For whole protein lysate preparation from A498 cells following stimulation, the medium was completely aspirated, the cells were washed once with PBS solution and 75 μL of cold lysis buffer (composition previously described [31]) was added to the cells, scraped and homogenised for 5 min in an ultrasonic bath. For human kidney samples, 100 μL of protein lysis buffer was used for homogenisation in an ultrasonic bath for 10 min. The human and cell culture lysates were centrifuged for 15 min at 17 000 *g*, the supernatant was collected and by using bicinchoninic acid protein assay kit (Pierce; Thermo Fisher Scientific) the protein concentration was determined. Twenty-five microgram of protein lysates were subjected to SDS gel electrophoresis (10% acrylamide gel), transferred onto a 0.45 μM nitrocellulose membrane (GE Healthcare; Amersham, UK; Thermo Fisher Scientific), blocked with 2.5% (w/v) non-fat milk and incubated with primary antibodies overnight at 4 °C. A secondary antibody against primary, conjugated to horseradish peroxidase and signal detection using luminol enhancer 32106 (Pierce; Thermo Fisher Scientific) was utilised to visualise protein bands. The antibodies used in this study include CTGF (sc365970, E-5 clone1220) (Santacruz, Heidelberg, Germany), S1P2 (Acris AP-01311, Herford, Germany), S1P3 (sc30024, Santacruz) and β-actin antibody (A-2228; Sigma Aldrich, St. Louis, MO, USA).

PRESTO-Tango assay

The PRESTO-Tango reporter activation assay was performed as described by Kroeze et al. [47] In concise, HTLA cells (HEK293 stable cell line expressing a tTA-dependent luciferase reporter and a β-arrestin2-TEV fusion gene) were seeded on Poly-L-Lysine (50 $\mu g \cdot mL^{-1}$ dissolved in PBS) coated P100 cell culture dishes and maintained in DMEM complete medium [supplemented with 10% FCS, puromycin (2 $\mu g \cdot mL^{-1}$), hygromycin (100 $\mu g \cdot mL^{-1}$)]. Transfection of S1PR-Tango constructs (Addgene plasmids gift from Bryan Roth, S1PR2-Tango #66497 and S1PR3-Tango #66498) was performed using Lipofectamine 2000 (Thermo Fisher Scientific). Twenty-four hours after transfection, cells were shifted onto a poly-L-Lysine coated 24-well plate (Greiner Bio-one, Kremsmünster, Austria) with HTLA selection medium. Cells were allowed to settle and were brought to quiescence by adding minimal medium overnight. Following starvation, the cells were treated with d16:1 S1P, d18:1 S1P or d20:1 S1P in different concentrations for 16 h. Finally, Luciferase activity was measured using the Dual-Luciferase Reporter

Assay System (E1910; Promega, Madison, WI, USA) on the GloMax Discover System (Promega) according to the company protocol. The luciferase luminescence readings from the instrument were normalised to protein values measured using Bradford protein assay.

Liquid chromatography/tandem mass spectrometry analysis

Measurement of Sphingolipids using liquid chromatography-tandem mass spectrometry in mice tissue, plasma and serum and human tissue samples was performed as described previously [31]. For sphingolipid measurements in tissue in mice, 8-week-old, male, C57BL/6J mice were purchased from Charles River, Sulzfeld, Germany.

Tissue/tumour samples used in this study were provided by the University Cancer Center Frankfurt (UCT). Written informed consent was obtained from all patients and the study was approved by the Institutional Review Boards of the UCT and the Ethical Committee at the University Hospital Frankfurt (project-number: UCT-12-2020). The distinction between tumour and normal tissue was made by a pathologist using instantaneous section diagnostics. Normal kidney tissue from the same patient was used as corresponding healthy control to tumour tissue.

Briefly, tissue samples were blended with 200 µL of extraction buffer (citric acid 30 mM, disodium hydrogen phosphate 40 mM) and spiked with 20 µL of the internal standard mixture (consisting of sphingosine d18:1-d7, sphinganine d18:0-d7, S1P d18:1-d7). Reference substances (sphingosine d18:1, sphingosine d20:1, sphinganine d18:0, sphinganine d20:0, S1P d18:1 and S1P d20:1) were purchased from Avanti Polar Lipids. Afterwards, samples were homogenised with methanol:chloroform: HCl (15:83:2, v/v/v) vortexed and centrifuged at 20 000 *g* for 5 min. The lower organic phase was evaporated under a gentle stream of nitrogen at 45 °C temperature and the residues were mixed with 100 µL methanol containing 5% formic acid and pipetted to glass vials. For calibration standards and quality control samples preparation, 20 µL of the working solution were processed as stated instead of sample.

The quantification of all analytes was performed using a hybrid triple quadrupole-ion trap mass spectrometer QTRAP 5500 (Sciex, Darmstadt, Germany) equipped with a Turbo-V-source operating in positive ESI mode. Sphingolipids were separated using an Agilent 1290 HPLC system equipped with a Zorbax C8 Eclipse Plus UHPLC column (2.1 * 30 mm, 1.8 µm; Agilent technologies, Waldbronn, Germany). Quality control samples at three different concentration levels (low, middle and high) were run at the beginning and end of each run. Samples were processed using Analyst software 1.6 and the obtained concentrations were evaluated using MultiQuant Software 3.0 (both Sciex, Toronto, Canada) using the internal standard method (isotope-dilution mass spectrometry). Calibration curves were calculated by linear or quadratic regression with $1/x$ weighting or $1/x^2$ weighting, respectively. Variations in the accuracy of the calibration standards were lower than 15% over the range of calibration, except for the lower limit of quantification (LLOQ), where a limit of 20% was accepted.

Statistical analysis

All statistical analyses were performed using GraphPad Prism (v6.01; GraphPad Software Inc., San Diego, CA, USA). We have first performed normality tests using D'Agostino and Pearson test for parametric distribution as well as the Kolmogorov–Smirnov test. All data with more than two groups were analysed by Kruskal–Wallis with Dunn's multiple-comparison test. Data are shown as box and whisker plots and shown as median ± IQR. In case of human samples, mRNA and sphingolipid levels line graphs were used and for the protein band analysis, box plots were used. For all experiments dealing with human samples, the Wilcoxon matched-pairs signed-rank test was used to calculate significance levels. A P-value < 0.05 was considered as statistically significant.

Acknowledgements

We would like to thank the University Cancer Center Frankfurt (UCT) for providing human samples. This work was supported by the German Research Foundation (SFB 1039) and Uniscientia Foundation (Vaduz) grants. We would also like to thank Prof. Dagmar Meyer zu Heringdorf for providing the S1PR-Tango constructs.

Conflict of interest

The authors declare no conflict of interest.

Author contributions

RV, MG, RB, AK designed and conducted experiments. MG, LS, JP, RB, WP analysed data and MG, RV, JP wrote the manuscript. ST and NB performed mass spectrometry.

Data availability statement

The data that support the findings of this study are available from the corresponding author, RV, upon reasonable request.

References

1 Hsieh JJ, Purdue MP, Signoretti S, Swanton C, Albiges L, Schmidinger M, et al. Renal cell carcinoma. *Nat Rev*

Dis Prim. 2017;**3**(1):17009. https://doi.org/10.1038/nrdp.2017.9
2 Errarte P, Larrinaga G, López JI. The role of cancer-associated fibroblasts in renal cell carcinoma. An example of tumor modulation through tumor/non-tumor cell interactions. *J Adv Res*. 2020;**21**:103–8. https://doi.org/10.1016/j.jare.2019.09.004
3 Boor P, Ostendorf T, Floege J. Renal fibrosis: novel insights into mechanisms and therapeutic targets. *Nat Rev Nephrol*. 2010;**6**(11):643–56.
4 Joung JW, Oh HK, Lee SJ, Kim YA, Jung HJ. Significance of intratumoral fibrosis in clear cell renal cell carcinoma. *J Pathol Transl Med*. 2018;**52**:323–30.
5 Hewitson TD. Renal tubulointerstitial fibrosis: common but never simple. *Am J Physiol Renal Physiol*. 2009;**296**(6):F1239–44. https://doi.org/10.1152/ajprenal.90521.2008
6 Nangaku M. Chronic hypoxia and tubulointerstitial injury: a final common pathway to end-stage renal failure. *J Am Soc Nephrol*. 2006;**17**(1):17–25.
7 López-Novoa JM, Rodríguez-Peña AB, Ortiz A, Martínez-Salgado C, López Hernández FJ. Etiopathology of chronic tubular, glomerular and renovascular nephropathies: clinical implications. *J Trans Med*. 2011;**9**(1):13.
8 Cox TR, Bird D, Baker A-M, Barker HE, Ho MW-Y, Lang G, et al. LOX-mediated collagen crosslinking is responsible for fibrosis-enhanced metastasis. *Can Res*. 2013;**73**(6):1721–32. https://doi.org/10.1158/0008-5472.CAN-12-2233
9 Steeg PS. Tumor metastasis: mechanistic insights and clinical challenges. *Nat Med*. 2006;**12**(8):895–904.
10 Mujtaba SS, Ni Y-B, Tsang JYS, Chan S-K, Yamaguchi R, Tanaka M, et al. Fibrotic focus in breast carcinomas: relationship with prognostic parameters and biomarkers. *Ann Surg Oncol*. 2013;**20**(9):2842–9. https://doi.org/10.1245/s10434-013-2955-0
11 Sánchez-López E, Rayego S, Rodrigues-Díez R, Rodriguez JS, Rodrigues-Díez R, Rodríguez-Vita J, et al. CTGF promotes inflammatory cell infiltration of the renal interstitium by activating NF-kappaB. *J Am Soc Nephrol*. 2009;**20**:1513–26.
12 Phanish MK, Winn SK, Dockrell MEC. Connective tissue growth factor-(CTGF, CCN2)–a marker, mediator and therapeutic target for renal fibrosis. *Nephron Exp Nephrol*. 2010;**114**(3):e83–92. https://doi.org/10.1159/000262316
13 Chen C-C, Lau LF. Functions and mechanisms of action of CCN matricellular proteins. *Int J Biochem Cell Biol*. 2009;**41**(4):771–83. https://doi.org/10.1016/j.biocel.2008.07.025
14 Lipson KE, Wong C, Teng Y, Spong S. CTGF is a central mediator of tissue remodeling and fibrosis and its inhibition can reverse the process of fibrosis. *Fibrogenesis Tissue Repair*. 2012;**5**:S24.
15 Ito Y, Aten J, Bende RJ, Oemar BS, Rabelink TJ, Weening JJ, et al. Expression of connective tissue growth factor in human renal fibrosis. *Kidney Int*. 1998;**53**(4):853–61. https://doi.org/10.1111/j.1523-1755.1998.00820.x
16 Cheng J-C, Wang EY, Yi Y, Thakur A, Tsai S-H, Hoodless PA. S1P stimulates proliferation by upregulating CTGF expression through S1PR2-mediated YAP activation. *Mol Cancer Res*. 2018;**16**(10):1543–55. https://doi.org/10.1158/1541-7786.MCR-17-0681
17 Lv L, Liu F-R, Na D, Xu H-M, Wang Z-N, Jiang C-G. Transforming growth factor-β1 induces connective tissue growth factor expression and promotes peritoneal metastasis of gastric cancer. *Biosci Rep*. 2020;**40**:BSR20201501. https://doi.org/10.1042/BSR20201501
18 Okusha Y, Eguchi T, Tran MT, Sogawa C, Yoshida K, Itagaki M, et al. Extracellular vesicles enriched with moonlighting metalloproteinase are highly transmissive, pro-tumorigenic, and trans-activates cellular communication network factor (CCN2/CTGF): CRISPR against cancer. *Cancers*. 2020;**12**(4):881. https://doi.org/10.3390/cancers12040881
19 Lucaciu A, Brunkhorst R, Pfeilschifter JM, Pfeilschifter W, Subburayalu J. The S1P–S1PR axis in neurological disorders-insights into current and future therapeutic perspectives. *Cells*. 2020;**9**(6):1515. https://doi.org/10.3390/cells9061515
20 Cartier A, Hla T. Sphingosine 1-phosphate: lipid signaling in pathology and therapy. *Science*. 2019;**366**(6463):eaar5551. https://doi.org/10.1126/science.aar5551
21 Baeyens AAL, Schwab SR. Finding a way out: S1P signaling and immune cell migration. *Annu Rev Immunol*. 2020;**38**(1):759–84. https://doi.org/10.1146/annurev-immunol-081519-083952
22 Alvarez SE, Milstien S, Spiegel S. Autocrine and paracrine roles of sphingosine-1-phosphate. *Trends Endocrinol Metab*. 2007;**18**(8):300–7. https://doi.org/10.1016/j.tem.2007.07.005
23 Takabe K, Spiegel S. Export of sphingosine-1-phosphate and cancer progression. *J Lipid Res*. 2014;**55**(9):1839–46. https://doi.org/10.1194/jlr.R046656
24 Kim RH, Takabe K, Milstien S, Spiegel S. Export and functions of sphingosine-1-phosphate. *Biochem Biophys Acta*. 2009;**1791**(7):692–6. https://doi.org/10.1016/j.bbalip.2009.02.011
25 Lucaciu A, Kuhn H, Trautmann S, Ferreirós N, Steinmetz H, Pfeilschifter J, et al. A sphingosine 1-phosphate gradient is linked to the cerebral recruitment of T helper and regulatory T helper cells during acute ischemic stroke. *Int J Mol Sci*. 2020;**21**:6242.
26 Galvani S, Sanson M, Blaho VA, Swendeman SL, Obinata H, Conger H, et al. HDL-bound sphingosine 1-phosphate acts as a biased agonist for the endothelial cell receptor S1P1 to limit vascular inflammation. *Sci Signal*. 2015;**8**:ra79.

27 Lowther J, Naismith JH, Dunn TM, Campopiano DJ. Structural, mechanistic and regulatory studies of serine palmitoyltransferase. *Biochem Soc Trans*. 2012;**40**:547–54.
28 Han G, Gupta SD, Gable K, Niranjanakumari S, Moitra P, Eichler F, et al. Identification of small subunits of mammalian serine palmitoyltransferase that confer distinct acyl-CoA substrate specificities. *Proc Natl Acad Sci USA*. 2009;**106**, 8186–91. https://doi.org/10.1073/pnas.0811269106
29 Hornemann T, Penno A, Rütti MF, Ernst D, Kivrak-Pfiffner F, Rohrer L, et al. The SPTLC3 subunit of serine palmitoyltransferase generates short chain sphingoid bases. *J Biol Chem*. 2009;**284**:26322–30.
30 Eliot AC, Kirsch JF. Pyridoxal phosphate enzymes: mechanistic, structural, and evolutionary considerations. *Annu Rev Biochem*. 2004;**73**:383–415.
31 Vutukuri R, Koch A, Trautmann S, Schreiber Y, Thomas D, Mayser F, et al. S1P d20:1, an endogenous modulator of S1P d18:1/S1P2 -dependent signaling. *FASEB J*. 2020;**34**:3932–42. https://doi.org/10.1096/fj.201902391R
32 Wang W, Xiang P, Chew WS, Torta F, Bandla A, Lopez V, et al. Activation of sphingosine 1-phosphate receptor 2 attenuates chemotherapy-induced neuropathy. *J Biol Chem*. 2020;**295**:1143–52.
33 Chua XY, Chai YL, Chew WS, Chong JR, Ang HL, Xiang P, et al. Immunomodulatory sphingosine-1-phosphates as plasma biomarkers of Alzheimer's disease and vascular cognitive impairment. *Alzheimers Res Ther*. 2020;**12**:122.
34 Troupiotis-Tsaïlaki A, Zachmann J, Gonzalez-Gil I, Wong AG, Ortega-Gutierrez S, López-Rodríguez ML, et al. Ligand chain length drives activation of lipid G protein-coupled receptors. *Sci Rep*. 2017;**7**:2020. https://doi.org/10.1038/s41598-017-02104-5
35 Cuvillier O, Pirianov G, Kleuser B, Vanek PG, Coso OA, Gutkind S, et al. Suppression of ceramide-mediated programmed cell death by sphingosine-1-phosphate. *Nature*. 1996;**381**:800–3.
36 Li M-H, Sanchez T, Pappalardo A, Lynch KR, Hla T, Ferrer F. Induction of antiproliferative connective tissue growth factor expression in Wilms' tumor cells by sphingosine-1-phosphate receptor 2. *Mol Cancer Res*. 2008;**6**:1649–56.
37 Katsuma S, Ruike Y, Yano T, Kimura M, Hirasawa A, Tsujimoto G. Transcriptional regulation of connective tissue growth factor by sphingosine 1-phosphate in rat cultured mesangial cells. *FEBS Lett*. 2005;**579**:2576–82.
38 Quehenberger O, Armando AM, Brown AH, Milne SB, Myers DS, Merrill AH, et al. Lipidomics reveals a remarkable diversity of lipids in human plasma. *J Lipid Res*. 2010;**51**:3299–305.
39 Maeda S, Shiimura Y, Asada H, Hirata K, Luo F, Nango E, et al. Endogenous agonist–bound S1PR3 structure reveals determinants of G protein–subtype bias. *Sci Adv*. 2021;**7**:eabf5325.
40 Wünsche C, Koch A, Goldschmeding R, Schwalm S, Dagmar Meyer Z, Heringdorf AH, et al. Transforming growth factor β2 (TGF-β2)-induced connective tissue growth factor (CTGF) expression requires sphingosine 1-phosphate receptor 5 (S1P5) in human mesangial cells. *Biochem Biophys Acta*. 2015;**1851**:519–26.
41 Xin C, Ren S, Kleuser B, Shabahang S, Eberhardt W, Radeke H, et al. Sphingosine 1-phosphate cross-activates the Smad signaling cascade and mimics transforming growth factor-beta-induced cell responses. *J Biol Chem*. 2004;**279**:35255–62.
42 O'Sullivan C, Dev KK. The structure and function of the S1P1 receptor. *Trends Pharmacol Sci*. 2013;**34**:401–12.
43 Huwiler A, Pfeilschifter J. Sphingolipid signaling in renal fibrosis. *Matrix Biol*. 2018;**68–69**:230–247. https://doi.org/10.1016/j.matbio.2018.01.006.
44 Ren S, Babelova A, Moreth K, Xin C, Eberhardt W, Doller A, et al. Transforming growth factor-beta2 upregulates sphingosine kinase-1 activity, which in turn attenuates the fibrotic response to TGF-beta2 by impeding CTGF expression. *Kidney Int*. 2009;**76**:857–67.
45 Koch A, Völzke A, Wünsche C, Meyer zu Heringdorf D, Huwiler A, Pfeilschifter J. Thiazolidinedione-dependent activation of sphingosine kinase 1 causes an anti-fibrotic effect in renal mesangial cells. *Br J Pharmacol*. 2012;**166**:1018–32.
46 Völzke A, Koch A, Meyer ZHD, Huwiler A, Pfeilschifter J. Sphingosine 1-phosphate (S1P) induces COX-2 expression and PGE2 formation via S1P receptor 2 in renal mesangial cells. *Biochem Biophys Acta*. 2014;**1841**:11–21. https://doi.org/10.1016/j.bbalip.2013.09.009
47 Kroeze WK, Sassano MF, Huang X-P, Lansu K, McCorvy JD, Giguère PM, et al. PRESTO-Tango as an open-source resource for interrogation of the druggable human GPCRome. *Nat Struct Mol Biol*. 2015;**22**:362–9.